

Cylindrical Relief Texture Mapping

Mohamed A. ElHelw

Guang-Zhong Yang

Department of Computing
Imperial College, 180 Queen's Gate,
SW7 2BZ, London, UK
{me|gzy}@doc.ic.ac.uk

ABSTRACT

This paper describes a new Image Based Rendering technique aimed at increasing the realism of textured cylindrical surfaces by adding 3D details and enhancing the depth conceived by the viewer. Cylindrical relief texture mapping extends the existing work on planar relief textures by using cylinders as warp surfaces. After mapping the planar relief texture to a reference cylinder, cylindrical warping equations are used to generate an intermediate image for texture mapping the reference cylinder and introducing motion parallax. The strength of the technique is demonstrated by the visual realism provided, with examples showing how the proposed method can be used for generating depth enhanced panoramas and improved endoscopic simulations.

Keywords

Image-Based Rendering, Image Warping, Range Images, Relief Textures, Texture Mapping.

1. INTRODUCTION

Over the last few years, image-based rendering (IBR) has established itself as a powerful alternative to conventional geometry-based computer graphics. A set of images or depth-enhanced images is used to synthesize novel views of either synthetic or real environments. The advantages of using image-based rendering methods include,

- Efficient representation, modeling and rendering of complex objects
- Sustained or enhanced system performance
- Increased rendering realism by accounting for global illumination and inter-object reflectance

The most familiar IBR method is texture mapping [Blin76], which is the first technique to represent complex materials that are hard to model and render. A major limitation of texture mapping is that texture mapped surfaces still appear as 2-D images painted onto flat polygons. They lack 3D details and don't exhibit appropriate parallax as the viewpoint changes. To address these problems, several extensions have been proposed over the years. Blinn [Blin78] developed a bump mapping technique that enables the surface to appear dimpled by applying perturbations to surface normals. The technique modifies the shading equation without affecting the real geometry. The results, however, are not always convincing especially when viewed from certain positions, as silhouette edges can appear to pass through depressions [Watt00]. Other methods such as displacement maps (rendered as mesh of micro polygons) and height fields proved either computationally prohibitive or not being able to handle situations where the depth values are considerably large compared to the surface being rendered. Better illusion of depth can be achieved at interactive rates by using image-based rendering methods, with which the texture image is associated with a depth map used in the image generation

Permission to make digital or hard copies of all or part of this work for personal or classroom use is granted without fee provided that copies are not made or distributed for profit or commercial advantage and that copies bear this notice and the full citation on the first page. To copy otherwise, or republish, to post on servers or to redistribute to lists, requires prior specific permission and/or a fee.

Journal of WSCG, Vol.11, No.1., ISSN 1213-6972
WSCG'2003, February 3-7, 2003, Plzen, Czech Republic.
Copyright UNION Agency – Science Press

process. This is referred to as image-based rendering by warping (IBRW) [Pope01].

Due to the fact that IBRW techniques can only warp depth-augmented images onto 2D planes, their applications are limited to planar polygons. The purpose of this work is to extend the previous work by Oliveira and Bishop [Oliv00b] for cylindrical relief texture mapping. Features of cylindrical relief texturing include:

- It adds 3D details and motion parallax to texture images mapped onto cylinders or surfaces enclosed by cylinders.
- It can be used to construct depth-enhanced panoramas that enable viewing complex scenes at interactive rates with enhanced realism and increased freedom of movement.
- It is suitable for a wide range of new applications that use closed surface models such as endoscopic simulation.

In the subsequent sections, we discuss previous work in 3D image-based rendering that is related to our method and describe the key stages involved in the cylindrical relief texture mapping process. Details about the derivation of the cylindrical warping equations are provided and the value of the proposed technique is demonstrated by two examples showing depth enhanced panoramas and endoscopic simulations.

2. PREVIOUS WORK

Image-based rendering techniques are becoming increasingly popular in recent years. While some image-based methods rely almost entirely on images to generate novel views [Levo96, Gort96, Shum99, Szel97], others depend on geometric or depth information about the scene being rendered [Blinn76, Rade99, Debe98]. In general, image-based rendering techniques can be classified into three main categories based on the amount of geometric information used: without geometry, implicit geometry and full geometry or depth methods [Shum00]. The technique presented here deals with images augmented with per-pixel depth information.

3D Image Warping [Mcmi97] maps visible points, each associated with a generalized disparity value, from source to target images. Along with the source camera model, the generalized disparity values provide a representation of the structure of the scene. A new image can be rendered from a nearby target viewpoint by projecting the source image pixels to their 3D positions and then re-projecting them onto

the target image plane. The 3D image warping equation is defined as [Mcmi97]:

$$\bar{x}_2 = \delta(x_1)M_2^{-1}(C_1 - C_2) + M_2^{-1}M_1\bar{x}_1$$

where $x_2(u_2, v_2)$ is the target image point coordinates, M_1 , C_1 , M_2 and C_2 define the source and target camera models respectively. In the above equation, $x_1(u_1, v_1)$ represents the source image point coordinates, and $\delta(x_1)$ the generalized disparity value at x_1 .

Shade *et al* [Shad98] describe the sprites with depth technique to provide enhanced parallax effects over ordinary sprites. An out-of-plane displacement component is added to each pixel in the sprite forming a displacement map. To avoid the usual problems related to forward mapping, *e.g.* filling holes and determining appropriate resampling, the displacement map is first forward mapped to the target view plane. The resulting map is then used with the inversely warped target view pixels and the epipole [Sawh94] of the target view to determine new pixel coordinates. Although this technique may look similar to relief texture mapping, there are intrinsic differences between the two [Oliv00b].

Debevec [Debe96] presents view-dependent texturing, an improved IBR texturing method aimed at increasing the realism of rendered geometric models. A set of images taken from different viewing angles for the same model is used. The images are projected onto the model using projective texture mapping [Debe98]. In the likely event that pixels from different images are projected to the same position, a fitness function is used to determine which image to be used. But as the best-fit image for a polygon is not fixed and can change from one pixel to another along the same polygon, a better solution to avoid the cause of seams is to combine pixels from several images to produce an averaged texture image according to weighting functions. The technique greatly enhances the realism of the rendered model as it accounts for the model reflectance changes caused by changing the viewing position in relation to the light sources and the 3D structure of the model.

The relief texture mapping introduced by Oliveira *et al* [Oliv00b] is based on simplified 1D versions of the 3D image warping equation [Mcmi97]. A relief texture image is warped (*i.e.* forward mapped) to a plane that has the same position and orientation as the target polygon in a pre-warping step. The generated image is then mapped onto the target polygon by

using the conventional texture mapping operation, which is also used for perspective image transformation and other image-related operations. The warping equations for relief textures mapping are given by [Oliv00a]:

$$u_2 = \frac{r}{t}, \quad v_2 = \frac{s}{t}$$

and

$$r = u_1 + k_1 \text{displ}(u_1, v_1),$$

$$s = v_1 + k_2 \text{displ}(u_1, v_1),$$

$$t = 1 + k_3 \text{displ}(u_1, v_1)$$

where (u_2, v_2) are target image point coordinates, (u_1, v_1) are source image point coordinates, and $\text{displ}(u_1, v_1)$ is the depth associated with source image point (u_1, v_1) . k_1 , k_2 and k_3 are constant coefficients for the current camera configuration.

Relief texture mapping adds 3D details to textured planar polygons and provides true view motion parallax. Its real strength originates from the fact that it can be incorporated into conventional polygonal systems and still offers the advantages of image-based rendering. Its main limitation is that it is only applicable to planar surfaces. In the described work, a different warping surface, *i.e.* a cylinder instead of a plane, is used. This resulted in a different mapping process and a new set of warping equations

The main processing steps involved in the proposed cylindrical relief texture mapping technique are schematically illustrated in Figure 1. First, a simple mapping from the planar relief texture space to a canonical cylindrical space is computed to get a cylindrical relief texture image. An intermediate image is then generated by warping the cylindrical relief texture image to its own basis by using the cylindrical warping equations. Finally, the intermediate image is texture mapped onto the used cylinder.

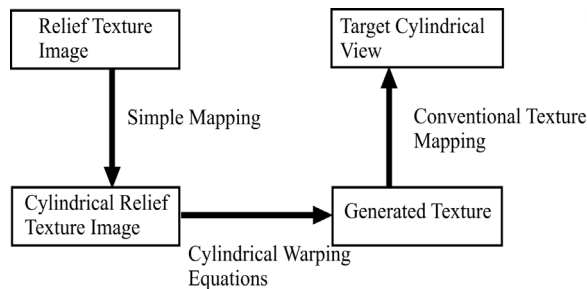


Figure 1. The three-stage mapping process of cylindrical relief texture mapping.

3. DERIVATION OF CYLINDRICAL WARPING EQUATIONS

Since a planar relief texture is a parallel projection image with center-of-projection (COP) at infinity, the first stage of the mapping process is to create a cylindrical relief texture image using simple mapping from planar to cylindrical spaces. In this case, image pixels along the horizontal direction (the u -direction) are projected to the same point on the axis of the cylinder, whereas pixels along the vertical direction are projected to different points along cylinder axis, as illustrated in Figure 2. By using this configuration, the center of projection of the cylindrical relief texture image is the axis of the cylinder.

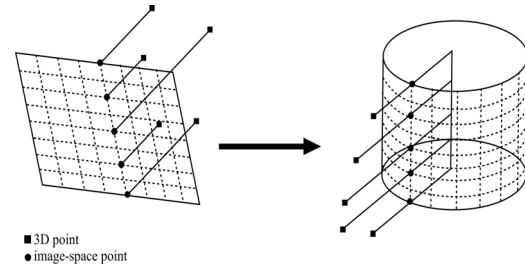


Figure 2. Simple mapping from planar to cylindrical relief texture. While the center-of-projection of a planar relief texture is at infinity, a cylindrical relief texture has its center-of-projection at the cylinder axis.

A point $b_s(u_s, v_s)$ of a cylindrical relief texture image with center-of-projection $C_s C'_s$, as shown in Figure 3, can be mapped to a 3D ray $\vec{r} = [r_x \ r_y \ r_z]^T$ using Equation (1):

$$\begin{bmatrix} r_x \\ r_y \\ r_z \end{bmatrix} = \begin{bmatrix} \cos(2\pi u_s) \\ 0 \\ \sin(2\pi u_s) \end{bmatrix} \quad (1)$$

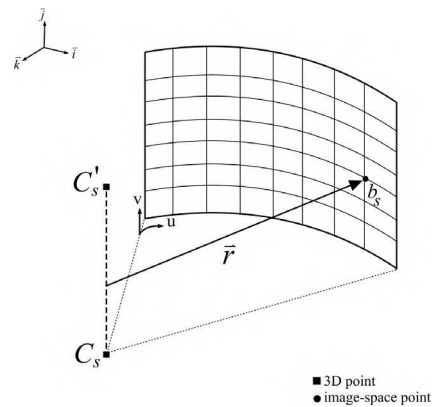


Figure 3. Mapping of cylindrical image-space point b_s to 3D-space ray r . All points along one image column result in the same 3D ray.

From Equation 1, all image points along one vertical direction, *i.e.* one image column, will result in the same 3D ray. Therefore, in order to warp a cylindrical relief texture, the warp is decomposed into horizontal and vertical warps that are performed sequentially in cylindrical image-space along the u and v directions. In this case, the cylindrical warping equations for both directions can be developed in 2D space with the advantages of simpler reconstruction and efficient execution.

The cylindrical warping equations compute the image of the cylindrical relief texture pixels on the reference cylinder as seen by a target viewpoint C_t . In other words, for a cylindrical relief texture image with center-of-projection $C_s C'_s$, the warping equations calculate the projection of image-space point $b_s(u_s, v_s)$ with associated depth $|\tilde{f}|$ ($|\tilde{f}|$ denotes the magnitude of \tilde{f}) onto the same cylinder based on target viewpoint C_t . This is illustrated in Figure 4. The resulting intermediate point $b_i(u_i, v_i)$ defines the shift in b_s coordinates due to the configuration of the target camera and the observed depth at b_s .

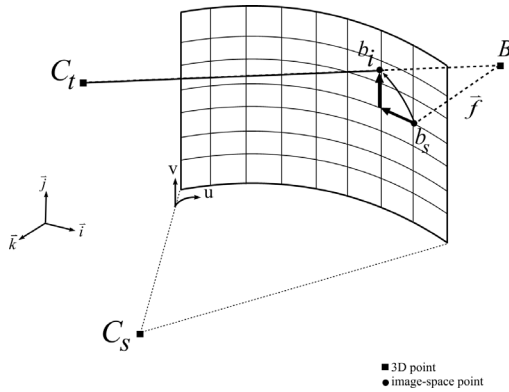


Figure 4. The cylindrical warping equations compute the shift of the cylindrical coordinates of point b_s to new point b_i induced by the position of target viewpoint C_t and the depth associated with b_s .

The Horizontal Warp

In order to compute the horizontal warp, we assume that the viewpoint C_t is at the center of a target cylinder as shown in Figure 5. The horizontal warp is then computed by first warping reference cylinder point u_s to target cylinder point u_t . This can be achieved by the following equations [Mcmi97]:

$$\begin{pmatrix} \cos(2\pi u_t) \\ \sin(2\pi u_t) \end{pmatrix} = \begin{pmatrix} \cos(2\pi u_s) \\ \sin(2\pi u_s) \end{pmatrix} + \delta(b_s) \begin{pmatrix} C_{sx} - C_{tx} \\ C_{sz} - C_{tz} \end{pmatrix} \quad (2)$$

and

$$u_t = \left(\frac{1}{2\pi} \right) \tan^{-1} \left(\frac{\sin(2\pi u_s) + \delta(b_s)(C_{sz} - C_{tz})}{\cos(2\pi u_s) + \delta(b_s)(C_{sx} - C_{tx})} \right) \quad (3)$$

where $\delta(b_s)$ is the generalized disparity value associated with reference image pixel b_s ; for a canonical cylinder, the generalized disparity is defined as: $\delta(b_s) = 1/(1+|\tilde{f}|)$

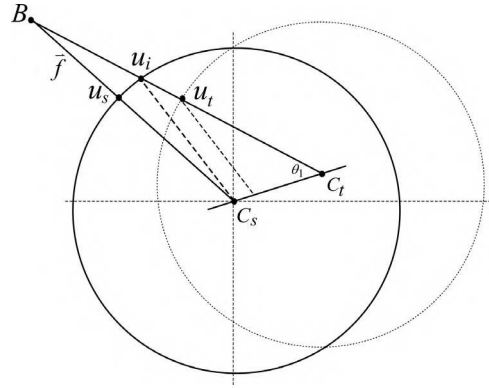


Figure 5. The horizontal warp calculates point b_s shift in the u -direction. A 2D warp, from the reference cylinder with center C_s to a target cylinder with center C_t , is carried out to get point u_t , which is used afterwards to compute u_i .

Then, the u -coordinate of the intermediate image point, u_i , is given as:

$$\begin{pmatrix} \cos(2\pi u_i) \\ \sin(2\pi u_i) \end{pmatrix} = \begin{pmatrix} \cos(2\pi u_t) \\ \sin(2\pi u_t) \end{pmatrix} + frac(b_s) \begin{pmatrix} C_{sx} - C_{tx} \\ C_{sz} - C_{tz} \end{pmatrix} \quad (4)$$

where $frac(b_s)$ is a fraction of the line segment connecting the reference and target cylinders centers, as shown in Figure 5. It is defined as, $frac(b_s) = \sin \theta_1 / \sin(\sin^{-1}(|C_s C_t| \sin \theta_1) + \theta_1)$. The details involving the calculation of $frac$ is given in the appendix. Expanding and rearranging Equation (4), we get the cylindrical warping equation for the horizontal warp as:

$$u_i = \left(\frac{1}{2\pi} \right) \left(\tan^{-1} \left[\frac{s}{t} \right] \right) \quad (5)$$

where,

$$s = \sin \left(\tan^{-1} \left(\frac{\sin(2\mu_i) + \delta(b_s)(C_{sz} - C_{tz})}{\cos(2\mu_i) + \delta(b_s)(C_{sx} - C_{tx})} \right) \right) + \text{frac}(b_s)(C_{sz} - C_{tz})$$

$$t = \cos \left(\tan^{-1} \left(\frac{\sin(2\mu_i) + \delta(b_s)(C_{sz} - C_{tz})}{\cos(2\mu_i) + \delta(b_s)(C_{sx} - C_{tx})} \right) \right) + \text{frac}(b_s)(C_{sx} - C_{tx})$$

It should be noted that the target cylinder (shown in dotted lines in Figure 5) is only used in the computation of u_i and it is the reference cylinder (shown in solid line in same the figure) that is texture mapped using the generated intermediate image in the last stage of the mapping process.

The Vertical Warp

Applying the horizontal warp to point $b_s(u_s, v_s)$ produces point $b'_s(u_i, v_s)$ which corresponds to source point shift along the horizontal image direction. The vertical warp is used afterwards to compute the vertical shift, that is from $b'_s(u_i, v_s)$ to $b_i(u_i, v_i)$.

The calculation of the vertical warp is similar to that of the planar case. From Figure (6b), it can be seen that

$$\tan \theta = (\nabla y) / (|\vec{f}|) = (y - \nabla y) / (L),$$

The displacement along the vertical warp, ∇y , can then be calculated as:

$$\nabla y = (|\vec{f}| * y) / (L + |\vec{f}|)$$

Given y in image-space coordinates, the intermediate point v-coordinate, v_i , is defined as:

$$v_i = v_s + \nabla y \quad (6)$$

It is worth noting that due to the curvature of the cylinder, the vertical warp is an approximation to the vertical shift. In most cases, the results are acceptable and will not cause noticeable distortions to the rendered images.

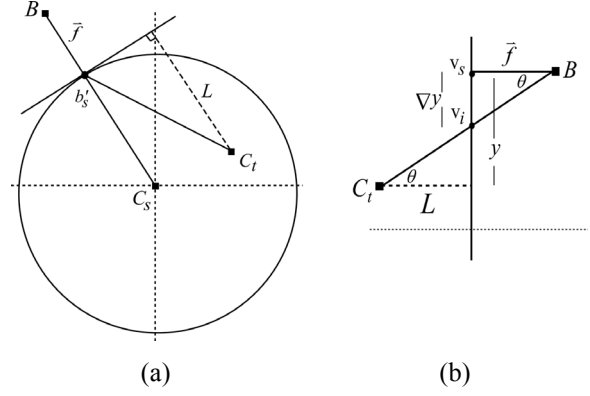


Figure 6. The vertical warp calculates point b'_s , vertical shift, that is from v_s to v_i , using simple geometry. The amount of shift is dependent on the orthogonal distance from the target viewpoint C_t to the plane tangent to cylinder at b'_s (6a) and the associated depth at b'_s . The geometry used to compute the vertical shift is shown in (6b).

4. RESULTS

To validate the proposed technique, depth-enhanced panoramas and endoscopic simulations with high fidelity visual realism have been used.

Depth-Enhanced Panoramas

The described technique can be used to generate improved panoramas. In conventional cylindrical panoramas [Chen95], an overlapping set of photographs taken from a camera rotating around its center point, are re-projected to cylindrical or spherical surfaces. These surfaces are used later to provide full 360-degree panoramic views [Pope01]. The user can view the scene interactively by changing the viewing orientation, while the viewing position is fixed. Although ordinary panoramas provide a fast interactive solution for viewing complex environments, the rendered images appear as flat surfaces mapped onto cylinders or spheres due to lack of depth.

Increased realism and more freedom of movement can be achieved using cylindrical relief texture mapping. By warping a relief texture image onto a cylinder and constraining camera motion within the cylinder, users experience convincing parallax effects provided by the depth of the relief texture. Compared to other IBR approaches [Chen95, Levo96, Gort96, Shum99], depth-enhanced panoramas provide more viewing space and require much less storage. Figure

7 shows two panoramic views of a section of the Roman Colosseum rendered without (7b) and with (7c) cylindrical relief texture mapping. In Figure 7c, it can be seen how the presented method adds to the visual realism of the rendered scene by highlighting the structure of 3D scene elements and improving the depth conceived by the viewer. This becomes more evident when the scene is viewed from a near position as shown in Figure 8.



(a)



(b)



(c)

Figure 7. Views from two panoramas of the Roman Colosseum. Views in (b) and (c) were generated without and with cylindrical relief texture mapping respectively. Notice the depth of arches and the 3D structure of columns in (c). Original planar relief texture image shown in (a).



Figure 8. The scene in the previous figure with cylindrical relief texture mapping as seen from a near viewpoint.

Endoscopic Simulations

Cylindrical relief texture mapping is well suited for endoscopic simulation because the surfaces used are closed surfaces. A surface-bounding cylinder is first computed as illustrated in Figure 9. The image is then warped using the bounding cylinder as the reference cylinder. Figure 10 shows two views of the same surface rendered without (a) and with (b) cylindrical relief texture mapping. In Figure 10b we can see how the 3D shape of the minute details on top of surface are emphasized along with the parallax between surface layers.

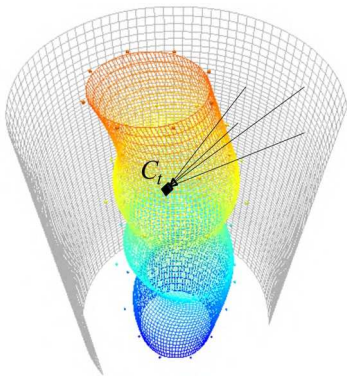
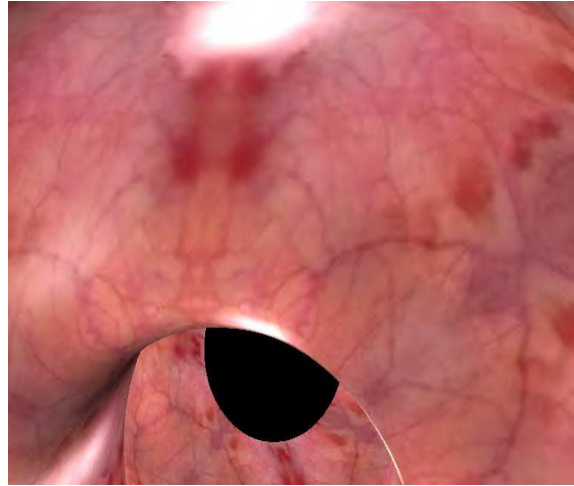


Figure 9. Cylindrical relief texture mapping can be used to enhance the realism of endoscopic simulations. A cylinder enclosing the surface is first computed then used in the cylindrical relief texture mapping process.

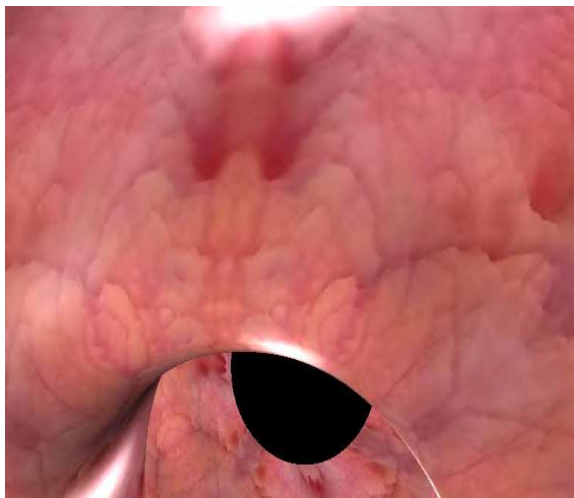
5. DISCUSSION AND FUTURE WORK

We have presented a novel IBR method based on warping relief textures onto cylinders. The process is composed of the following steps: A simple mapping from the relief texture space to cylindrical space is used to get a cylindrical relief texture image. It is then warped by using the cylindrical warping equations to generate an intermediate image that is finally texture mapped onto the target surface. Based on the proposed technique, we introduced depth-enhanced panoramas, a new image-based rendering modality, that provides better visual realism and more freedom of movement while requiring minimal storage. We also discussed technique application to endoscopic simulations.

One major limitation of the cylindrical relief texture mapping technique is that it supports only one depth value along each line of sight. Therefore, artifacts appear when occluded parts of the original surface become visible. Moreover, the technique cannot correctly handle surfaces with multiple layers.



(a)



(b)

Figure 10. The use of cylindrical relief texture mapping emphasizes the 3D shape of tiny details and enhances parallax between surface layers. This becomes notable the more the viewpoint gets closer to the surface (cylindrical relief texture mapping used in 10b).

While some work has been done to address this problem for planar relief textures [Pari02], resolving it for cylindrical relief texture mapping is a topic to be explored. Further research is to be carried out on the modification of the cylindrical warping equations so that planar relief texture images can be mapped onto general cylinders instead of only right cylinders as this will lead to a significant improvement in the quality of generated imagery when the technique is used in endoscopic simulation. Additional area for investigation is the use of dynamic shading [Oliv98] in the case cylindrical relief texture mapping.

6. REFERENCES

- [Blin76] Blinn J. F., Newell M. E. Texture and Reflection in Computer Generated Images. CACM, Vol.19, No 10, pp. 542-547, 1976.
- [Blin78] Blinn, J. Simulation of Wrinkled Surfaces. In Proc. Siggraph78, pp. 286-292, 1978.
- [Chen95] Chen, S. E. QuickTime VR – an image-based approach to virtual environment navigation. Computer Graphics, pp. 29–38, 1995.
- [Debe96] Debevec, P. E., Taylor, C. J., and J. Malik. Modeling and rendering architecture from photographs: A hybrid geometry and image-based approach. Computer Graphics, pp. 11–20, 1996.
- [Debe98] Debevec, P., Yu, Y., and Borshukov, G. Efficient view-dependent image-based rendering with projective texture-mapping. In Proc. 9th Eurographics Workshop on Rendering, pp. 105–116, 1998.
- [Gort96] Gortler, S. J., Grzeszczuk, R., Szeliski, R., and Cohen, M. F. The lumigraph. In Computer Graphics Proceedings, Annual Conference Series, pp. 43–54, 1996.
- [Levo96] Levoy, M., and Hanrahan, P. Light Field Rendering. In Proc SIGGRAPH 96, pp. 31-42, 1996.
- [Mcmi97] McMillan, L. An Image-Based Approach to Three-Dimensional Computer Graphics. Ph.D. Dissertation, UNC Computer Science Technical Report TR97-013, 1997.
- [Oliv98] Oliveira, M., and Bishop, G. Dynamic Shading in Image-Based Rendering. UNC TR98-023, University of North Carolina, 1998.
- [Oliv00a] Oliveira, M. Relief Texture Mapping. Ph.D. Dissertation. UNC Computer Science Technical Report TR00-009, 2000.
- [Oliv00b] Oliveira, M., Bishop, G. and McAllister, D. Relief Texture Mapping. In Proc. SIGGRAPH 00, pp. 231-242, 2000.
- [Pope01] Popescu, V. Forward Rasterization: A Reconstruction Algorithm for Images-Based Rendering. Ph.D. Dissertation. UNC TR01-019, University of North Carolina, 2001.
- [Pari02] Parilov, S. and Stuerzlinger, W. Layered Relief Textures. Journal of WSCG, Vol. 10, No. 2, ISSN 1213-6972, pp. 357-364, 2002.
- [Rade99] Rademacher, P. View-dependent geometry. In Proc SIGGRAPH 1999, pp. 439–446, 1999.
- [Sawh94] Sawhney, H. S. 3D Geometry from Planar Parallax. In IEEE Computer Society Conference on Computer Vision and Pattern Recognition (CVPR'94), pp. 929–934, 1994.
- [Shad98] Shade, J., Gortler, S., He, L.-W and Szeliski, R. Layered Depth Images. In Proc. SIGGRAPH 98, pp.231-242, 1998.
- [Shum99] Shum, H.-Y. and He, L.-W. Rendering with concentric mosaics. In Proc. SIGGRAPH 99, pp. 299–306, 1999.
- [Shum00] Shum, H-Y. and Kang, S.B. A Review of Image-based Rendering Techniques. IEEE/SPIE Visual Communications and Image Processing, pp. 2-13, 2000.
- [Szel97] Szeliski, R. and Shum, H.-Y. Creating full view panoramic image mosaics and texture-mapped models. In Computer Graphics, pp. 251–258, 1997.
- [Watt00] Watt, A. 3D Computer Graphics. 3rd Edition. Addison Wesley, 2000.

APPENDIX Calculation of *frac*

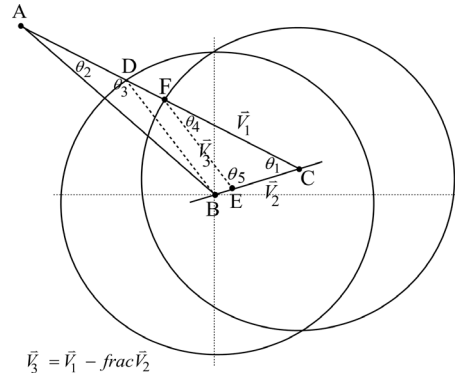


Figure 11. Geometry used for calculating *frac*

Figure 11 shows the reference and target cylindrical images from a top view. Points B and C are in place of reference and target image centers of projection respectively. From the figure we have.

$$\frac{\sin \theta_1}{AB} = \frac{\sin \theta_2}{BC} \Delta ABC \quad \sin \theta_2 = BC \sin \theta_1 / AB$$

$$\frac{\sin \theta_3}{AB} = \frac{\sin \theta_2}{1} \Delta ADB \quad \sin \theta_3 = AB \sin \theta_2 = BC \sin \theta_1$$

$$\sin \theta_4 = \sin \theta_3 = BC \sin \theta_1 \quad \frac{\sin \theta_4}{EC} = \sin \theta_5 \Delta CEF$$

$$\theta_5 = \theta_3 - \theta_1 \quad \sin \theta_5 = \sin^{-1}(BC \sin \theta_1 + \theta_1)$$

Solving for *frac* we get:

$$EC = \frac{\sin \theta_4}{\sin \theta_5} = \frac{BC \sin \theta_1}{\sin(\sin^{-1}(BC \sin \theta_1 + \theta_1))}$$

$$frac = EC / BC = \frac{\sin \theta_1}{\sin(\sin^{-1}(BC \sin \theta_1 + \theta_1))}$$